

An adaptive reduced basis ANOVA method for high-dimensional Bayesian inverse problems

Qifeng Liao^a, Jinglai Li^{b,*}

^a School of Information Science and Technology, ShanghaiTech University, Shanghai 201210, China

^b Department of Mathematical Sciences, University of Liverpool, Liverpool L69 7XL, UK

ARTICLE INFO

Article history:

Received 20 November 2018

Received in revised form 13 April 2019

Accepted 24 June 2019

Available online 5 July 2019

Keywords:

ANOVA

Reduced basis methods

Bayesian inference

Markov Chain Monte Carlo

Inverse problems

ABSTRACT

In Bayesian inverse problems sampling the posterior distribution is often a challenging task when the underlying models are computationally intensive. To this end, surrogates or reduced models are often used to accelerate the computation. However, in many practical problems, the parameter of interest can be of high dimensionality, which renders standard model reduction techniques infeasible. In this paper, we present an approach that employs the ANOVA decomposition method to reduce the model with respect to the unknown parameters, and the reduced basis method to reduce the model with respect to the physical parameters. Moreover, we provide an adaptive scheme within the MCMC iterations, to perform the ANOVA decomposition with respect to the posterior distribution. With numerical examples, we demonstrate that the proposed model reduction method can significantly reduce the computational cost of Bayesian inverse problems, without sacrificing much accuracy.

© 2019 Elsevier Inc. All rights reserved.

1. Introduction

Inverse problems arise from many fields of science and engineering—whenever parameters of interest must be estimated from indirect observations [1]. The Bayesian inference method has become increasingly popular as a tool to solve inverse problems [2,3]. The popularity of the method is largely due to its ability to quantify the uncertainty in the solution obtained. Simply speaking, in the Bayesian framework, the parameters of interest are cast as random variables to which a prior distribution is assigned, and then the posterior distribution of the parameters conditional on the observed data is computed via the Bayes' rule. The posterior distribution thus provides a probabilistic characterization of the parameters of interest in such problems.

Though the idea behind the Bayesian inference method is quite straightforward, the computation of the posterior distribution often poses challenges. In most practical problems, the posterior distributions do not admit a closed-form expression and must be computed numerically. To this end, the Markov chain Monte Carlo (MCMC) method [4] is often used to compute the posterior distributions. In particular, the MCMC method draws samples from the posterior distribution and then any posterior statistics can be evaluated with the obtained samples. As will be shown later, the MCMC method requires to repeatedly evaluate the likelihood function and each evaluation involves a full simulation of the forward function, i.e., the mapping from the parameter of interest to the observables. In many practical problems, such as the seismic inversion [5] and the inverse groundwater modelling [6], the forward functions are often described by computationally intensive partial

* Corresponding author.

E-mail addresses: liaoqf@shanghaitech.edu.cn (Q. Liao), Jinglai.Li@liverpool.ac.uk (J. Li).

differential equations (PDEs). On the other hand, often a rather large number of samples are required to accurately estimate certain posterior moments. In this case, the total cost of the MCMC simulation may become prohibitively high.

To improve the overall computational efficiency of the MCMC simulation, we can reduce either the number of samples required or the cost for generating each sample. The first option is essentially to develop more efficient sampling schemes, which is not in the scope of this work. We here consider the second option, i.e., to reduce the cost for computing each sample. To this end, a natural idea is to construct computationally inexpensive surrogates/reduced models and use them in the MCMC procedure. Substantial efforts have been made toward this direction and various types of surrogate models have been used to approximate the forward functions, most notably, the polynomial chaos expansion (PCE) [7–13], the Gaussian process surrogates [14–16], the sparse grid interpolation [17,18], and the reduced order models (ROM) [19–24]. The performances of these methods (especially the PCE and the ROM) for accelerating the Bayesian computation is detailedly compared and discussed in [25].

The surrogate or reduced model based methods have been successfully applied to a large variety of inverse problems, resulting in significant computational saving of the Bayesian inference. Despite the success, the applicability of these methods is often ultimately limited by the dimensionality of the unknown parameters. In many real-world applications, the unknown parameters are often of very high dimensionality: for example, in groundwater modelling one may want to estimate the hydraulic conductivity, and in seismic inversion it is the wave velocity that one is interested in; in these problems, the unknowns are spatial fields, and if we represent the unknown fields with mesh grid points, the resulting inverse problems can be of tens of thousands or more dimensions. Doing Bayesian inference directly for such problems is often not possible, and in practice it often requires dimension reduction for the input space to make the inference feasible. In particular, the truncated Karhunen–Loeve (KL) expansion is often used to represent the unknown field that we want to estimate [8,26] to reduce the dimensionality. However, in many practical problems, the unknown fields are rough, and in this case one still needs to use a rather large number of KL modes to represent it. Constructing surrogate or reduced models for such high-dimensional problems directly is a rather challenging task.

The main purpose of this work is to provide an approach to tackle the dimensionality issue and construct reduced models for such problems. Specifically, we focus on the Analysis of Variance (ANOVA) methods [27–32]. The ANOVA methods, which are proposed for efficiently solving high-dimensional forward uncertainty quantification (UQ) problems, aim to decompose a high-dimensional parameter space into a union of low-dimensional spaces, such that standard surrogate/reduced modelling strategies can be applied. For example, these include ANOVA based stochastic collocation [33,34], ANOVA multi-element collocation [35], and reduced basis ANOVA [36–38]. However, how to develop an efficient ANOVA approach for high-dimensional Bayesian inversion still remains an open question. The main difficulty here is that, conducting ANOVA decomposition of high-dimensional models requires the knowledge of the distribution of the input parameters, which in the Bayesian inverse problems is the posterior that we want to compute. An approximate solution is to perform ANOVA decomposition with respect to the prior distribution, but the prior based ANOVA decomposition is often inefficient, especially when the prior is significantly different from the posterior. Thus, we develop an adaptive reduced basis ANOVA (RB-ANOVA) algorithm which allows us to construct a reduced model with respect to the posterior distribution, which, as is illustrated by numerical examples, is more efficient than that constructed based on the prior. To summarize, the main contributions of this work are two-fold: first we propose to use the RB-ANOVA model to accelerate the MCMC simulations for high-dimensional Bayesian inverse problems; second, we develop an adaptive scheme to construct the RB-ANOVA model with respect to the posterior distribution.

The rest of the paper is organized as follows. In Section 2 we describe the formulation of the Bayesian inverse problems that will be considered in this work. In Section 3 we provide a scheme for constructing the RB-ANOVA model, and in Section 4 we present our new RB-ANOVA based Markov chain Monte Carlo (RB-ANOVA-MCMC) algorithm, which adaptively constructs the RB-ANOVA model with respect to the posterior distribution within the MCMC iterations. In Section 5, with numerical experiments we demonstrate that the proposed adaptive RB-ANOVA method can significantly accelerate the Bayesian computation. Finally some concluding remarks are offered in Section 6.

2. Bayesian inverse problems

In this section we describe the problem setup that is used in this work. Suppose that we are interested in an M -dimensional parameter $\xi = [\xi_1, \dots, \xi_M]^T \in \mathbb{R}^M$, and we want to estimate it from some observed data d . Moreover we assume that there exists a forward model G that maps the unknown parameter ξ to the data d :

$$d = G(\xi) + \epsilon, \quad (1)$$

where ϵ is the measurement noise. Let $\pi_\epsilon(\epsilon)$ be the distribution of ϵ , and one can obtain the distribution of d conditional on ξ :

$$\pi(d|\xi) = \pi_\epsilon(d - G(\xi)). \quad (2)$$

In a Bayesian formulation, one assigns a prior distribution $\pi(\xi)$ on ξ encoding the prior knowledge on the parameter of interest, and the posterior $\pi(\xi|d)$ can then be calculated via Bayes' rule:

$$\pi(\xi|d) = \frac{\pi(d|\xi)\pi(\xi)}{\int \pi(d|\xi)\pi(\xi)d\xi}, \quad (3)$$

where the denominator is a normalization constant that makes the posterior a well-defined probability distribution. We note here that, in practice it is usually reasonable to assume that the sought parameters are in a (sufficiently large) bounded region, and thus in this paper, we shall restrict our attention to the situation that the prior $\pi(\xi)$ has a bounded and connected support. Without loss of generality, we then assume the support of $\pi(\xi)$ is I^M where $I := [-1, 1]$ throughout this work.

As is mentioned earlier, one frequently employs the MCMC simulation to sample the posterior distribution. Simply speaking, the MCMC method constructs a Markov chain which asymptotically converges to the posterior distribution. In this work, we adopt the popular Metropolis-Hastings (MH) MCMC algorithm outlined in Algorithm 1, to generate N samples $\{\xi^{(1)}, \dots, \xi^{(N)}\}$ of the posterior of ξ . In Algorithm 1, $\pi(\cdot|\xi^{(j)})$ on line 3 is a given proposal distribution which may be a multivariate normal distribution with mean $\xi^{(j)}$, and $U[0, 1]$ on line 5 refers to the uniform distribution on $[0, 1]$.

Algorithm 1 The standard MH algorithm.

```

1: Initialize the chain at  $\xi^{(1)}$ .
2: for  $j = 1 : N - 1$  do
3:   Draw  $\xi^* \sim \pi(\cdot|\xi^{(j)})$ .
4:   Compute the acceptance ratio  $a = \min\left(1, \frac{\pi_\epsilon(d-G_J(\xi^*))\pi(\xi^*)}{\pi_\epsilon(d-G_J(\xi^{(j)}))\pi(\xi^{(j)})} \frac{\pi(\xi^{(j)}|\xi^*)}{\pi(\xi^*|\xi^{(j)})}\right)$ .
5:   Draw  $\rho \sim U[0, 1]$ .
6:   if  $\rho < a$  then
7:     Let  $\xi^{(j+1)} = \xi^*$ .
8:   else
9:     Let  $\xi^{(j+1)} = \xi^{(j)}$ .
10:  end if
11: end for
```

It can be seen from the algorithm that, each MCMC iteration requires an evaluation of the computationally expensive forward function $G(\cdot)$ (on line 4 of Algorithm 1), which renders the MCMC procedure formidably expensive. In what follows we provide a reduced basis ANOVA based method to accelerate the MCMC computation.

3. The RB-ANOVA method

To begin with, details of the forward model considered in this paper are addressed as follows. Let D denote a spatial domain (a subset of \mathbb{R}^2 or \mathbb{R}^3) which is bounded, connected and with a polygonal boundary ∂D , and $x \in D$ denote a spatial variable. The physics of problems considered are governed by a PDE over the spatial domain D and boundary conditions on the boundary ∂D , which are stated as: find $u(x, \xi)$ mapping $D \times I^M$ to \mathbb{R} , such that

$$\mathcal{L}(x, \xi; u(x, \xi)) = f(x) \quad \forall (x, \xi) \in D \times I^M, \quad (4a)$$

$$\mathfrak{b}(x, \xi; u(x, \xi)) = g(x) \quad \forall (x, \xi) \in \partial D \times I^M, \quad (4b)$$

where \mathcal{L} is a partial differential operator and \mathfrak{b} is a boundary operator, both of which can depend on the unknown parameter ξ . Here f is the source function and g specifies the boundary conditions. Through specifying an observation operator c , e.g., taking solution values at several grid points, we write the overall forward model as $G(\xi) := c(u(x, \xi))$. It is clear that each evaluation of the forward function requires to solve the PDE (4), and this procedure needs to be performed repeatedly in the MCMC iterations. As discussed earlier, we shall construct computationally inexpensive reduced models and use them in the MCMC iteration to accelerate the computation. However, when the parameter of interest is high-dimensional, constructing reduced models are rather challenging. In this work, the ANOVA decomposition approach is used to decompose the model so that the reduced model construction becomes feasible. The construction of the RB-ANOVA surrogate for the forward models is discussed in this section, which is an extension of the procedure outlined in [37], and the application of it to Bayesian inversion is presented in the next section.

3.1. ANOVA decomposition

We present the ANOVA decomposition method in a generic setting. Namely, suppose that we have a computationally intensive function $u(x, \xi)$ where $x \in D$ is the physical variable and $\xi \in I^M$ is the random variable, and the goal here is to construct a reduced model (or approximation) of $u(x, \xi)$ with respect to the random variable ξ .

To proceed, the notation for indices are first set up following [31,37]. In general, any subset of $\{1, \dots, M\}$ denotes an index. For an index $t \subseteq \{1, \dots, M\}$, $|t|$ denotes the cardinality of t , and we define $|t| = 0$ for $t = \emptyset$. For an index $t \neq \emptyset$, we sort its elements in ascending order and express it as $t = (t_1, \dots, t_{|t|})$ with $t_1 < t_2 \dots < t_{|t|}$. In addition, we also call $|t|$ the (ANOVA) order of t , and call t a $|t|$ -th order index. For a given ANOVA order $i = 0, \dots, M$, the following index sets are defined

$$\begin{aligned}\mathfrak{T}_i &:= \{t \mid t \subset \{1, \dots, M\}, |t| = i\}, \\ \mathfrak{T}_i^* &:= \cup_{j=0,1,\dots,i} \mathfrak{T}_j, \\ \mathfrak{T} &:= \mathfrak{T}_M^* = \cup_{j=0,1,\dots,M} \mathfrak{T}_j.\end{aligned}$$

The sizes of the above sets (numbers of elements that they contain) are denoted by $|\mathfrak{T}_i|$, $|\mathfrak{T}_i^*|$ and $|\mathfrak{T}|$ respectively. From the above definition, $\mathfrak{T}_0 = \{\emptyset\}$ and $|\mathfrak{T}_0| = 1$. For a given index $t = (t_1, \dots, t_{|t|}) \in \mathfrak{T}$ with $|t| > 0$, ξ_t denotes a random vector collecting components of ξ associated with t , i.e., $\xi_t := [\xi_{t_1}, \dots, \xi_{t_{|t|}}]^T \in I^{|t|}$, and we denote the (marginal) prior probability density function of ξ_t by $\pi_t(\xi_t)$ and its (marginal) posterior probability density function by $\pi_t^*(\xi_t) := \pi_t(\xi_t|d)$.

While noting that there are other strategies to implement the ANOVA decomposition [33,34,39], here we adopt the so-called anchored ANOVA method following [33,34,32,37]. In this method, one first selects an anchor point $c = [c_1, \dots, c_M]^T \in I^M$, and then decomposes the function $u(x, \xi)$ with respect to $\xi = [\xi_1, \dots, \xi_M]^T \in I^M$ as,

$$\begin{aligned}u(x, \xi) &= u_0(x) + u_1(x, \xi_1) + \dots + u_{1,2}(x, \xi_{1,2}) + \dots \\ &= \sum_{t \in \mathfrak{T}} u_t(x, \xi_t),\end{aligned}\tag{5}$$

where we denote $u_\emptyset(x, \xi_\emptyset) := u_0(x)$ for convenience, and each term in (5) is specified as

$$u_\emptyset(x, \xi_\emptyset) := u_0(x) := u(x, c),\tag{6a}$$

$$u_t(x, \xi_t) := u(x, c, \xi_t) - \sum_{s \subset t} u_s(x, \xi_s).\tag{6b}$$

In the equation above, we have $\xi_\emptyset = c$, and $u(x, c, \xi_t)$ is defined as,

$$u(x, c, \xi_t) := u(x, \xi^{c,t}),$$

where

$$\xi^{c,t} := [\xi_1^{c,t}, \dots, \xi_M^{c,t}]^T,\tag{7a}$$

$$\xi_i^{c,t} := \begin{cases} c_i & \text{for } i \in \{1, \dots, M\} \setminus t \\ \xi_i & \text{for } i \in t \end{cases}.\tag{7b}$$

In what follows, $u_t(x, \xi_t)$ is called a *child term* of $u_s(x, \xi_s)$ if $s \subset t$. It should be clear that the decomposition (5) is exact and so itself does not provide us a reduced model of the solution $u(x, \xi)$. However, as discussed in [33,34,37], an efficient reduced model can be obtained if one only keeps a small number of *active* terms in (5). We will discuss how to select the active terms later. For now supposing that we have selected the active terms, the sets consisting of selected important indices at each order are denoted by $\mathcal{J}_i \subseteq \mathfrak{T}_i$ for $i = 0, \dots, M$. We then define $\mathcal{J}_i^* := \cup_{j=0,1,\dots,i} \mathcal{J}_j$ and $\mathcal{J} := \mathcal{J}_M^*$. A reduced model of the solution $u(x, \xi)$ is obtained:

$$u(x, \xi) \approx u_{\mathcal{J}}(x, \xi) := \sum_{t \in \mathcal{J}} u_t(x, \xi_t),\tag{8}$$

where u_t is defined in (6b). In the following, $u_{\mathcal{J}}(x, \xi)$ is called the ANOVA model (or approximation) of $u(x, \xi)$.

For selecting the active terms (or indices) in the ANOVA model, the prior distribution π_t of ξ_t is given in advance in this Bayesian inference setting, and thus a natural idea is to construct the selection criterion using some prior statistics. While they are not optimal choices, the prior statistics are used to illustrate the methods in this section, and optimal selection criteria based on posterior distributions are presented in our new algorithm in the next section. To this end, we adopt the relative mean approach used in [37], while noting that other choices are also possible [33,34]. Specifically, recalling that the prior mean of u_t is

$$\mathbf{E}(u_t) := \int_{I^{|t|}} u_t(x, \xi_t) \pi_t(\xi_t) d\xi_t,$$

we define the relative mean value to be

$$\gamma_t := \frac{\|\mathbf{E}(u_t)\|_{0,D}}{\left\| \sum_{s \in \mathcal{J}_{|t|-1}^*} \mathbf{E}(u_s) \right\|_{0,D}},$$

where $\|\cdot\|_{0,D}$ denotes the L^2 function norm over region D . In practice, the prior expectation $\mathbf{E}(u_t)$ can be computed with a Monte Carlo (MC) estimator:

$$\tilde{\mathbf{E}}(u_t) := \frac{1}{N} \sum_{j=1}^N u_t(x, \xi_t^{(j)}), \quad (9)$$

where $\{\xi_t^{(j)}\}_{j=1}^N$ are N samples drawn from π_t , and as a result, the relative mean value γ_t can be approximated by

$$\gamma_t := \frac{\|\tilde{\mathbf{E}}(u_t)\|_{0,D}}{\left\|\sum_{s \in \mathcal{J}_{|t|-1}^*} \tilde{\mathbf{E}}(u_s)\right\|_{0,D}}. \quad (10)$$

Here we call a term u_t *important* if the associated relative mean estimate is larger than a prescribed threshold value tol_{anova} . The set of active terms at each order is selected with the following procedure. Namely, suppose that \mathcal{J}_i is given, and one first selects all important terms at order i , yielding the index set

$$\tilde{\mathcal{J}}_i := \{t \mid t \in \mathcal{J}_i \text{ and } \gamma_t \geq tol_{anova}\},$$

which is a subset of \mathcal{J}_i . After that, as discussed in [33], the index set at order $i+1$ is constructed by

$$\mathcal{J}_{i+1} := \left\{ t \mid t \in \mathcal{J}_i, \text{ and any } s \subset t \text{ with } |s| = i \text{ satisfies } s \in \tilde{\mathcal{J}}_i \right\}. \quad (11)$$

That is, if a term is found unimportant, the term itself is not removed from the ANOVA model, but all its child terms are removed for the next order. To start the procedure, we set $\tilde{\mathcal{J}}_0 = \mathcal{J}_0 = \mathcal{T}_0 = \emptyset$. On the other hand, the procedure terminates automatically if no active term is found for the next order. The studies in [33,34] indicate that for most realistic physical systems the size of \mathcal{J} is usually much smaller than that of \mathcal{T} , and moreover, \mathcal{J} may only contain low order terms.

3.2. The RB approximation

In the present problem, $u(x, \xi)$ is the solution of the parameterized equation (4). As mentioned in the previous section, the ANOVA decomposition method yields a reduced model in the random parameter space. Here we discuss how to perform model reduction with respect to the physical parameter x , with the reduced basis (RB) method.

First, to use the ANOVA model (8), the terms $u(x, c, \xi_t)$ in (6) for all $t \in \mathcal{J}$ need to be computed. Here, $u(x, c, \xi_t)$ is the solution of the following equations:

$$\mathcal{L}_t(x, \xi_t; u(x, c, \xi_t)) = f(x) \quad \forall (x, \xi_t) \in D \times I^{|t|}, \quad (12a)$$

$$\mathfrak{b}_t(x, \xi_t; u(x, c, \xi_t)) = g(x) \quad \forall (x, \xi_t) \in \partial D \times I^{|t|}, \quad (12b)$$

where $u(x, c, \xi_t)$ is defined by (7) and \mathcal{L}_t and \mathfrak{b}_t are defined through putting (7) into (4). Eqs. (12) are referred to as a (parametrically) $|t|$ -dimensional *local* problem, while the global problem is Eqs. (4). It is easy to see that, if $u(x, c, \xi_t)$ is evaluated by directly solving the local problem (12) with the same strategy for solving (4), evaluating the ANOVA model (8) is actually much more expensive than solving the global problem (4) directly. This is because that the ANOVA model requires to solve the local problem multiple times and a full solve of the local problem is about as costly as that of the global problem. Thus, to make the ANOVA model useful for our problem, a reduced model for the local problem (12) needs to be constructed, so that it can be solved more efficiently. We construct such a model using the RB method.

We start with the finite element approximation of the local problem (12). In general, the variational form of the deterministic problem (12) corresponding to a given realization of ξ_t is given by $\mathfrak{B}_{\xi_t}(u(x, c, \xi_t), v) = l(v)$. Given a finite element space X^h with N_h degrees of freedom, a finite element formulation seeks a solution $u^h(x, c, \xi_t) \in X^h$ such that

$$\mathfrak{B}_{\xi_t}(u^h(x, c, \xi_t), v) = l(v), \quad \forall v \in X^h. \quad (13)$$

As usual, a finite element solution u^h is referred to as a *snapshot*. Next, the reduced basis (RB) approximation is stated as: given a set of reduced basis functions $Q_t := \{q_t^{(1)}, \dots, q_t^{(N_r)}\} \subset X^h$, find $u^r(x, c, \xi_t) \in \text{span}\{Q_t\}$ such that

$$\mathfrak{B}_{\xi_t}(u^r(x, c, \xi_t), v) = l(v), \quad \forall v \in \text{span}\{Q_t\}. \quad (14)$$

Two standard methods are used to generate the reduced bases Q_t for all $t \in \mathcal{J}$ in this paper. The first one is the proper orthogonal decomposition (POD) [40–42], which can be briefly reviewed as follows. For a given finite sample set $\Xi \subset I^{|t|}$ with size $|\Xi|$, a finite snapshot set is defined by

$$S_{\Xi}^t := \left\{ u^h(x, c, \xi_t), \xi_t \in \Xi \right\}. \quad (15)$$

The matrix form of S_{Ξ}^t is denoted by $\mathbf{S}_{\Xi}^t \in \mathbb{R}^{N_h \times |\Xi|}$, i.e., each column of \mathbf{S}_{Ξ}^t is the vector of basis function coefficients of a finite element solution. Assuming $|\Xi| < N_h$, let $\mathbf{S}_{\Xi}^t = U \Sigma V^T$ denote the singular value decomposition (SVD) of \mathbf{S}_{Ξ}^t , where

$U = (\mathbf{q}_1, \dots, \mathbf{q}_{|\Xi|})$ and $\Sigma = \text{diag}(\sigma_1, \dots, \sigma_{|\Xi|})$ with $\sigma_1 \geq \sigma_2 \geq \dots \geq \sigma_{|\Xi|} \geq 0$. The basis Q_t is then given by the first k left singular vectors $(\mathbf{q}_1, \dots, \mathbf{q}_k)$, of which the corresponding singular values are greater than some given tolerance tol_{pod} , i.e., $\sigma_k/\sigma_1 > \text{tol}_{\text{pod}}$ but $\sigma_{k+1}/\sigma_1 \leq \text{tol}_{\text{pod}}$. As usual, to simplify the later presentation, this POD procedure for generating Q_t through S_Ξ^t is denoted by $Q_t := \text{POD}(S_\Xi^t)$.

The second one is the greedy sampling method [43–49]. This method is to adaptively select parameter samples, where errors between the reduced approximation and the finite element approximation are large. To assess the errors, we use the residual error indicator which is also adopted by [50,37,51,52]. Following our notation in [50], when considering linear PDEs, the algebraic system associated with (13) can be written as $\mathbf{A}_{\xi_t} \mathbf{u}_{\xi_t} = \mathbf{f}$ where $\mathbf{A}_{\xi_t} \in \mathbb{R}^{N_h \times N_h}$, and $\mathbf{u}_{\xi_t}, \mathbf{f} \in \mathbb{R}^{N_h}$. The algebraic system of the reduced basis approximation (14) can be written as $\mathbf{Q}_t^T \mathbf{A}_{\xi_t} \mathbf{Q}_t \tilde{\mathbf{u}}_{\xi_t} = \mathbf{Q}_t^T \mathbf{f}$, where $\tilde{\mathbf{u}}_{\xi_t} \in \mathbb{R}^{N_r}$ gives a reduced basis solution and $\mathbf{Q}_t \in \mathbb{R}^{N_h \times N_r}$ is the matrix form of the reduced basis $Q_t = \{q_1, \dots, q_{N_r}\}$, i.e., each column of \mathbf{Q}_t is the vector of nodal coefficient values associated with each q_i , $i = 1, \dots, N_r$. The residual indicator is defined by

$$\tau_{\xi_t} := \frac{\|\mathbf{A}_{\xi_t} \mathbf{Q}_t \tilde{\mathbf{u}}_{\xi_t} - \mathbf{f}\|_2}{\|\mathbf{f}\|_2}. \quad (16)$$

Note that through storing some precomputed matrices, the cost of computing the residual indicator is $O(N_r^2)$ (see [50] for details), while it may not be a certified estimator (see [43,48,49] for detailed analysis of a posteriori error estimation for reduced basis methods). With this residual indicator, the greedy sampling procedure can be stated as follows. First, take the first sample $\xi_t^{(1)}$ from a given sample set Ξ and initialize the reduced basis as $Q_t := \{u^h(x, c, \xi_t^{(1)})\}$. Second, for each $\xi_t \in \Xi$, compute the residual error indicator τ_{ξ_t} using the current reduced basis Q_t , and if τ_{ξ_t} is larger than some given tolerance, compute the snapshot $u^h(x, c, \xi_t)$ and augment Q_t with $u^h(x, c, \xi_t)$. The second step is repeated until N_r snapshots are obtained.

3.3. The RB-ANOVA model

With the local problem (12) solved by the RB method, we obtain a RB-ANOVA model:

$$u_{\mathcal{J}}^r(x, \xi) := \sum_{t \in \mathcal{J}} u_t^r(x, \xi_t), \quad (17)$$

where

$$u_{\emptyset}^r(x, \xi_{\emptyset}) := u^h(x, c), \quad (18a)$$

$$u_t^r(x, \xi_t) := u^r(x, c, \xi_t) - \sum_{s \subset t} u_s^r(x, \xi_s). \quad (18b)$$

In (18), $u^r(x, c, \xi_t)$ is the RB solution of the local problem (14), and $u^h(x, c)$ is the snapshot at the anchor point (i.e., the solution of (13) with $t = \emptyset$). Constructing the RB-ANOVA model in our setting is equivalent to generating four pieces of data: the anchor point c , the snapshot $u^h(x, c)$ at the anchor point, the index set \mathcal{J} , and the reduced basis Q_t for each $t \in \mathcal{J}$. We call these data the RB-ANOVA model data. With them, a RB-ANOVA approximation $u_{\mathcal{J}}^r(x, \xi)$ at any input sample point $\xi \in I^M$ can be cheaply computed. The procedures for generating the RB-ANOVA data $\{c, u^h(x, c), \mathcal{J}, \{Q_t\}_{t \in \mathcal{J}}\}$ are as follows.

First, suppose that we are given a set of realizations of the random variable ξ , denoted by Ξ . As discussed in [31], for a given distribution of ξ , the optimal anchor point c with respect to this distribution is its mean point. However, the goal of this work is to generate samples for the posterior distribution, of which the exact mean point is not admitted. As an alternative, the anchor point in this work is taken to be the sample mean of Ξ .

We set $\mathcal{J}_0 := \{\emptyset\}$, and compute the snapshot $u^h(x, c)$. The zeroth order RB is constructed using this snapshot $Q_{\emptyset} := \{u^h(x, c)\}$, and the mean estimate for the zeroth order ANOVA term is set to $\bar{E}(u_{\emptyset}) := u^h(x, c)$. Moreover, it is easy to see that $\tilde{\mathcal{J}}_0 = \mathcal{J}_0$, which immediately implies that $\mathcal{J}_1 := \{1, \dots, M\}$. Now we consider an ANOVA order $i \geq 1$. That is, given the index set \mathcal{J}_i and the reduced bases for order $i-1$, $\{Q_s\}_{s \in \mathcal{J}_{i-1}}$, we need to find the set $\tilde{\mathcal{J}}_i$ and the reduced bases $\{Q_t\}_{t \in \mathcal{J}_i}$. Now recall that, the set $\tilde{\mathcal{J}}_i$ is obtained by estimating the relative means with MC approximation. It should be clear that here if the Monte Carlo samples of $\{u_t(x, \xi_t^{(j)})\}_{j=1}^N$ for each $t \in \mathcal{J}_i$ are computed with the PDE model with finite elements, the total cost may become prohibitively high. To reduce the cost, we consider the reduced basis MC method which incorporates greedy RB methods in MC simulations [47], and extend it to yield both the set $\tilde{\mathcal{J}}_i$ and the reduced bases $\{Q_t\}_{t \in \mathcal{J}_i}$ with low costs.

To start the greedy procedure, the hierarchical approach introduced in [37] is used to initialize the reduced basis Q_t for $t \in \mathcal{J}_i$, which reuses the bases generated at the previous order based on the nested structure of ANOVA indices:

- grouping all reduced basis functions associated with subindices of t with order $|t|-1$ together, we define $Q_t^0 := \cup_{s \in \Lambda_t} Q_s$ where $\Lambda_t := \{s \mid s \in \mathcal{J}_{|t|-1} \text{ and } s \subset t\}$;

2. we apply POD to Q_t^0 to result in an orthogonal basis to serve as an initialization of Q_t , i.e., we initially set $Q_t := \text{POD}(Q_t^0)$ (details of POD are discussed in Section 3.2).

After the initial basis is generated, a sample set of ξ_t for $t \in \mathcal{J}_i$ needs to be specified to conduct the MC simulation. Since the sample set Ξ is given for the global parameter ξ and each ξ_t for $t \in \mathcal{J}$ is a collection of components of ξ , it is trivial to define a sample set of ξ_t by a collection of the components of samples in Ξ , i.e., the samples of ξ_t are taken to be $\Xi_t := \{\xi_t^{(j)}, \xi^{(j)} \in \Xi \text{ for } j = 1, \dots, |\Xi|\} \subset I^{|t|}$. Then, looping over the sample points, we compute the reduced solution $u^r(x, c, \xi_t^{(j)})$ (see (14)) for each $\xi_t^{(j)} \in \Xi_t$, and the residual indicator $\tau_{\xi_t^{(j)}}$ (see (16)):

1. if the residual indicator is smaller than a given tolerance tol_{rb} , use $u^r(x, c, \xi_t^{(j)})$ to serve as a MC solution sample;
2. if the residual indicator is larger than or equal to tol_{rb} , compute the snapshot $u^h(x, c, \xi_t^{(j)})$ through solving (13), use the snapshot to serve as a MC solution sample and update the reduced basis Q_t with this snapshot.

When all $|\Xi_t|$ MC samples are generated through the above greedy approach, we compute the relative mean values using (10) and construct the important index set $\tilde{\mathcal{J}}_i$, which consequently yields \mathcal{J}_{i+1} . As is mentioned in Section 3.1, the above procedure is repeated until $\mathcal{J}_{i+1} = \emptyset$. This RB-ANOVA procedure is formally stated in Algorithm 2. It should be noted that this algorithm only requires a set of realizations of ξ , Ξ , as its input, and this is an important property for the adaptive algorithm that will be presented in the next section. We also note that, a major difference between Algorithm 2 and that developed in [37] is that, in [37] the RB-ANOVA model is constructed with the tensor grid collocation points, while here MC samples are used. The sensitivity criterion (line 22 of Algorithm 2) is computed through the Monte Carlo mean estimate (9), where the solution samples are computed on line 14 and line 17 of Algorithm 2. So, there is no extra PDE evaluation involved on line 22 of Algorithm 2, and the cost of computing the sensitivity criterion is equivalent to the cost of computing the Monte Carlo mean estimate (9) using $|\Xi_t|$ existing samples.

Algorithm 2 Constructing the RB-ANOVA model.

```

1: Input: a finite sample set  $\Xi := \{\xi^{(j)}, j = 1, \dots, |\Xi|\} \subset I^M$ .
2: Compute the anchor point  $c := \frac{1}{|\Xi|} \sum_{j=1}^{|\Xi|} \xi^{(j)}$ .
3: Set  $\mathcal{J}_0 := \{\emptyset\}$ , compute  $u^h(x, c)$  (see (13)) and set  $u_\emptyset(x, \xi_\emptyset) := u^h(x, c)$ .
4: Set  $Q_\emptyset := \{u^h(x, c)\}$ ,  $\tilde{\mathbf{E}}(u_\emptyset) := u^h(x, c)$ .
5: Set  $\mathcal{J}_1 := \{1, \dots, M\}$ , initialize  $\mathcal{J} := \mathcal{J}_0 \cup \mathcal{J}_1$ , and let  $i = 1$ .
6: while  $\mathcal{J}_i \neq \emptyset$  do
7:   for  $t \in \mathcal{J}_i$  do
8:     Construct  $Q_t^0 := \cup_{s \in \Lambda_t} Q_s$  where  $\Lambda_t := \{s | s \in \mathcal{J}_{[t]-1} \text{ and } s \subset t\}$ .
9:     Initialize  $Q_t := \text{POD}(Q_t^0)$ , (see Section 3.2 for details of the POD method).
10:    Construct the sample set  $\Xi_t := \{\xi_t^{(j)}, \xi^{(j)} \in \Xi \text{ for } j = 1, \dots, |\Xi|\} \subset I^t$ .
11:    for  $j = 1 : |\Xi_t|$  do
12:      Compute the reduced solution  $u^r(x, c, \xi_t^{(j)})$  through solving (14) and the error indicator  $\tau_{\xi_t^{(j)}}$  through (16).
13:      if  $\tau_{\xi_t^{(j)}} < tol_{rb}$  then
14:        Set  $u(x, c, \xi_t^{(j)}) = u^r(x, c, \xi_t^{(j)})$  in (6b) to obtain  $u_t(x, \xi_t^{(j)})$ .
15:      else
16:        Compute the snapshot  $u^h(x, c, \xi_t^{(j)})$  (see (13)).
17:        Set  $u(x, c, \xi_t^{(j)}) = u^h(x, c, \xi_t^{(j)})$  in (6b) to obtain  $u_t(x, \xi_t^{(j)})$ .
18:        Augment the reduced basis  $Q_t$  with  $u^h(x, c, \xi_t^{(j)})$ , i.e.  $Q_t = Q_t \cup \{u^h(x, c, \xi_t^{(j)})\}$ .
19:      end if
20:    end for
21:    Compute  $\tilde{\mathbf{E}}(u_t)$  using (9) with samples  $\{u_t(x, \xi_t), \xi_t \in \Xi_t\}$ .
22:    Compute the relative mean value  $\tilde{\gamma}_t = \left\| \tilde{\mathbf{E}}(u_t) \right\|_{0,D} / \left\| \sum_{s \in \mathcal{J}_{i-1}} \tilde{\mathbf{E}}(u_s) \right\|_{0,D}$ .
23:  end for
24:  Set  $\tilde{\mathcal{J}}_i := \{t | t \in \mathcal{J}_i, \text{ and } \tilde{\gamma}_t \geq tol_{anova}\}$ .
25:  Set  $\mathcal{J}_{i+1} := \{t | t \in \mathcal{J}_{i+1}, \text{ and any } s \subset t \text{ satisfies } s \in \tilde{\mathcal{J}}_i\}$ .
26:  Update the index set  $\mathcal{J} := \mathcal{J} \cup \mathcal{J}_{i+1}$  and update  $i = i + 1$ .
27: end while
28: Output ANOVA model data:  $\{c, u^h(x, c), \mathcal{J}, \{Q_t\}_{t \in \mathcal{J}}\}$ .

```

We next discuss how to use the resulting RB-ANOVA model (17) to predict the system output $G(\xi)$ for an arbitrary input sample of ξ , as is required in the MCMC iterations. First, we set $u_\emptyset^r(x, \xi_\emptyset) := u^h(x, c)$ as (18a). Second, the reduced basis approximation $u^r(x, c, \xi_t)$ of the solution of each local system (12) for $t \in \mathcal{J}$ is computed through solving (14) with the reduced basis Q_t . After that, $u_t^r(x, \xi_t)$ is computed through (18b), and the overall reduced basis ANOVA approximation $u_{\mathcal{J}}^r(x, \xi)$ are computed through (17). Finally, applying the given observation operator c on $u_{\mathcal{J}}^r(x, \xi)$, the overall system output is estimated, i.e., we denote $G_{\mathcal{J}}^r(\xi) := c(u_{\mathcal{J}}^r(x, \xi))$. This prediction procedure is summarized in Algorithm 3.

Algorithm 3 Predication via reduced basis ANOVA model.

```

1: Input: a sample of  $\xi$  and the RB-ANOVA model data  $\{c, u^h(x, c), \mathcal{J}, \{Q_t\}_{t \in \mathcal{J}}\}$ .
2: Set  $u_\emptyset^r(x, \xi_0) := u^h(x, c)$ .
3: for  $t \in \mathcal{J} \setminus \{\emptyset\}$  do
4:   Compute  $u^r(x, c, \xi_t)$  through solving (14) with the reduced basis  $Q_t$ .
5:   Obtain  $u_t^r(x, \xi_t)$  through (18b).
6: end for
7: Assemble  $u_{\mathcal{J}}^r(x, \xi)$  using (17).
8: Set  $G_{\mathcal{J}}^r(\xi) := c(u_{\mathcal{J}}^r(x, \xi))$  where  $c$  is the given observation operator.
9: Output:  $G_{\mathcal{J}}^r(\xi)$ .

```

4. The adaptive RB-ANOVA method to accelerate MCMC

In Section 3.3, the schemes for constructing and using the RB-ANOVA surrogate for the forward models are presented. In the MCMC iterations, the computationally intensive finite element method can be replaced with the RB-ANOVA model to reduce the computational cost. As discussed in Section 3.3, a simple way of doing this is to construct the RB-ANOVA model with respect to the prior distribution before performing the MCMC simulation, which means that the sample set used to construct the reduced model in Algorithm 2 is generated from the prior distribution $\pi(\xi)$. An issue here is that, the goal of the Bayesian inference is to sample according to the posterior distribution, and in this case, constructing the reduced model with respect to the prior distribution may become ineffective, especially for problems in which the posterior differs significantly from the prior [53]. Ideally one should construct the reduced model with respect to the posterior distribution for such problems, but this certainly can not be done in advance as the posterior is not available in advance. To address the issue, we here present an algorithm that can adaptively construct the RB-ANOVA model according to the posterior distribution. Specifically, the new method updates the RB-ANOVA model inside the MCMC iterations, and for conciseness we shall refer to the whole procedure as the RB-ANOVA-MCMC algorithm in the following.

In this section, the number of samples for generating the RB-ANOVA model is denoted by N_{model} , i.e., $|\Xi| = N_{\text{model}}$ on line 1 of Algorithm 2. To begin with, we construct an initial RB-ANOVA model using Algorithm 2 with N_{model} samples drawn from the prior distribution $\pi(\xi)$, and start the MCMC iterations with this initial model. Initializing a Markov chain $\Xi^* := \{\xi^{(1)}\}$ where $\xi^{(1)}$ is a sample from the prior $\pi(\xi)$, for each $j \geq 1$, we first draw a candidate sample ξ^* from a proposal distribution which is denoted by $\pi(\cdot | \xi^{(j)})$, and evaluate the system output corresponding to $\xi^{(j)}$ using Algorithm 3, which is denoted by $G_{\mathcal{J}}^r(\xi^{(j)})$. After that, a Metropolis acceptance ratio is computed through

$$a := \min \left(1, \frac{\pi_\epsilon(d - G_{\mathcal{J}}^r(\xi^*)) \pi(\xi^*)}{\pi_\epsilon(d - G_{\mathcal{J}}^r(\xi^{(j)})) \pi(\xi^{(j)})} \frac{\pi(\xi^{(j)} | \xi^*)}{\pi(\xi^* | \xi^{(j)})} \right). \quad (19)$$

With probability a , the candidate sample is accepted, i.e., $\xi^{(j)} := \xi^*$; otherwise, the candidate sample is rejected, i.e., $\xi^{(j)} := \xi^{(j-1)}$. The Markov chain is then augmented with $\xi^{(j)}$, i.e., $\Xi^* = \Xi^* \cup \xi^{(j)}$. After N_{model} posterior samples are generated, the RB-ANOVA model is updated—the RB-ANOVA model data $\{c, u^h(x, c), \mathcal{J}, \{Q_t\}_{t \in \mathcal{J}}\}$ are reconstructed using Algorithm 2 with these N_{model} posterior samples. The MCMC procedure continues with the new RB-ANOVA model. The RB-ANOVA model is reconstructed periodically every N_{model} MCMC iterations, until certain stopping conditions are satisfied. Namely, as the number of MCMC samples increases, it is expected that the resulting RB-ANOVA model may not vary much. Thus, we terminate the reconstruction procedure if the new model data and current model data are similar. Specifically, the index set \mathcal{J} is used to serve as the stopping criterion: the model reconstruction procedure is stopped if the new and the current index sets are the same.

This new adaptive RB-ANOVA-MCMC procedure is formally presented in Algorithm 4. In the inputs of this algorithm, N refers to the desired number of posterior samples to generate, and N_{model} is the sample size to generate the RB-ANOVA model. The variable *Update_Label* is used to label whether to stop updating the RB-ANOVA model during the MCMC iterations.

Finally, we provide some discussions on how the use of the posterior distribution may improve the performance of the model reduction. The improvement is two-fold: it improves the efficiency of both the ANOVA model (for the random parameters) and the reduced basis model (for the physical parameters). First, for the ANOVA model, both the anchor point and the important terms are selected based on some statistical moments of the random parameters. In particular, it has been discussed in [31] that the efficiency of an ANOVA expansion depends critically on the choice of the anchor point—to achieve a given level of accuracy, a properly chosen anchor point can lead to a small number of expansion terms in (5) or (17), and they have suggested that an effective choice of the anchor point is the mean of the random parameters [31]. Moreover, the active terms of the ANOVA model are also selected using the relative means. In a Bayesian problem, the random parameters are essentially distributed according to the posterior rather than the prior, and thus estimating these moments with respect to the posterior distribution should yield a much more accurate ANOVA representation than that with the prior. On the other hand, constructing the input sample set to generate the RB-ANOVA model from the posterior can also improve the performance of the reduced basis model and the argument here is similar as that in [53,19]: since the RB functions are chosen with respect to the input samples, constructing input samples from the posterior can ensure

that the basis functions are mostly distributed in the high probability regions of the posterior, and the resulting RB model may be of higher accuracy in those regions. We will demonstrate that the proposed method can significantly improve the performance in Section 5.

Algorithm 4 The adaptive RB-ANOVA-MCMC algorithm.

```

1: Input:  $N$  and  $N_{\text{model}}$ .
2: Compute the RB-ANOVA model data  $\{c, u^h(x, c), \mathcal{J}, \{Q_t\}_{t \in \mathcal{J}}\}$  using Algorithm 2 with  $N_{\text{model}}$  samples drawn from the prior distribution  $\pi(\xi)$ .
3: Draw a sample  $\xi^{(1)}$  from the prior, and initialize the Markov chain  $\Xi^* := \{\xi^{(1)}\}$ .
4: Let  $\text{Update\_Label} := 1$ .
5: for  $j = 1, \dots, N - 1$  do
6:   Draw  $\xi^* \sim \pi(\cdot | \xi^{(j)})$ .
7:   Compute the RB-ANOVA output  $G_{\mathcal{J}}^r(\xi^*)$  using Algorithm 3.
8:   Compute the acceptance ratio

$$a = \min \left( 1, \frac{\pi_\epsilon(d - G_{\mathcal{J}}^r(\xi^*)) \pi(\xi^*)}{\pi_\epsilon(d - G_{\mathcal{J}}^r(\xi^{(j)})) \pi(\xi^{(j)}) \pi(\xi^* | \xi^{(j)})} \right).$$

9:   Draw  $\rho \sim U[0, 1]$ .
10:  if  $\rho < a$  then
11:    Let  $\xi^{(j+1)} = \xi^*$ .
12:  else
13:    Let  $\xi^{(j+1)} = \xi^{(j)}$ .
14:  end if
15:  if  $j \bmod N_{\text{model}} = 0$  and  $\text{Update\_Label} = 1$  then
16:    Store the current ANOVA index set  $\mathcal{J}' = \mathcal{J}$ .
17:    Update the RB-ANOVA model data  $\{c, u^h(x, c), \mathcal{J}, \{Q_t\}_{t \in \mathcal{J}}\}$  using Algorithm 2 with the last  $N_{\text{model}}$  samples in the chain  $\{\xi^{(j-N_{\text{model}}+1)}, \dots, \xi^{(j)}\} \subset \Xi^*$ .
18:    if  $\mathcal{J}$  is the same as  $\mathcal{J}'$  then
19:      Stop future RB-ANOVA model updates through setting  $\text{Update\_Label} := 0$ .
20:    end if
21:  end if
22: end for

```

5. Numerical study

The numerical examples considered are steady flows in porous media. Letting $a(x, \xi)$ denote a unknown permeability field and $u(x, \xi)$ the pressure head, we consider the following diffusion equation,

$$-\nabla \cdot (a(x, \xi) \nabla u(x, \xi)) = 1 \quad \text{in } D \times I^M, \quad (20a)$$

$$u(x, \xi) = 0 \quad \text{on } \partial D \times I^M, \quad (20b)$$

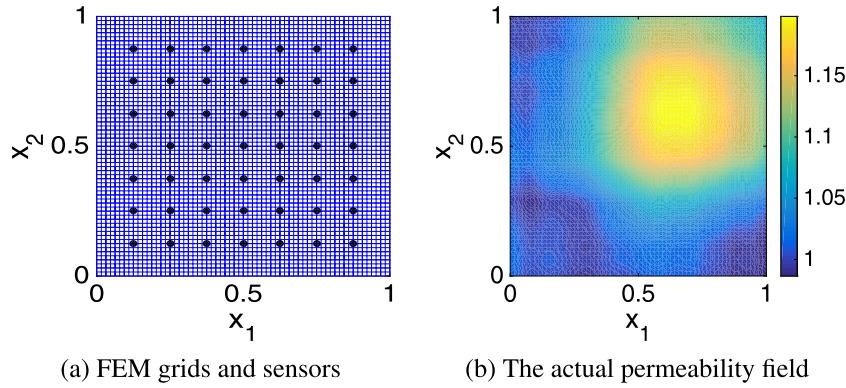
where $D \subset \mathbb{R}^2$ and the dimension of the parameter M is specified when we parameterize the permeability field next. Given a realization of ξ , defining $H^1(D) := \{u : D \rightarrow \mathbb{R}, \int_D u^2 dD < \infty, \int_D (\partial u / \partial x_1)^2 dD < \infty \text{ and } \int_D (\partial u / \partial x_2)^2 dD < \infty\}$ and $H_0^1(D) := \{v \in H^1(D) | v = 0 \text{ on } \partial D\}$, the weak form of (20) is to find $u(x, \xi) \in H_0^1(D)$ such that $(a \nabla u, \nabla v) = (1, v)$ for all $v \in H_0^1(D)$. We discretize in space using a bilinear finite element approximation [54,55]. The spatial domain in the following numerical studies is taken to be $D = (0, 1) \times (0, 1)$. The problem is discretized in space on a uniform 65×65 grid (the number of the spatial degrees of freedom is $N_h = 4225$). Our deterministic forward model $G(\xi)$ is defined to be a set collecting solution values corresponding to measurement sensors— $\{u(x, \xi), \xi \in \mathbf{d}\}$ where the sensor set \mathbf{d} in this work is defined to be the tensor product $\{x_i\} \otimes \{y_i\}$ of the one-dimensional grids: $x_i = 0.125i$, $y_i = 0.125i$, for $i = 1, \dots, 7$. We set the measurement noise ϵ in (1) to independent and identically distributed Gaussian distributions with mean zero and standard deviation 0.001. Fig. 1 shows locations of sensors with the finite element grids and the true permeability field used to generate the test data.

We parameterize the permeability field $a(x, \xi)$ by a truncated Karhunen–Loëve (KL) expansion [56–58] of a random field with mean function $a_0(x)$, standard deviation σ and covariance function

$$\text{Cov}(x, y) = \sigma^2 \exp \left(-\frac{|x_1 - y_1|}{\alpha} - \frac{|x_2 - y_2|}{\alpha} \right), \quad (21)$$

where α is the correlation length. The KL expansion is expressed as

$$a(x, \xi) = a_0(x) + \sum_{k=1}^M \sqrt{\lambda_k} a_k(x) \xi_k, \quad (22)$$

**Fig. 1.** Setup of the numerical test.

where $\{\xi_k\}_{k=1}^M$ are random variables, M is the number of KL modes retained, $a_k(x)$ and λ_k are the eigenfunctions and eigenvalues of (21). We set $a_0(x) = 1$ and $\sigma = 0.25$ in the numerical studies. The priori distributions of $\{\xi_k\}_{k=1}^M$ are set to independent uniform distributions with range $I = [-1, 1]$. Different values of the correlation length α are studied. As usual, we set M large enough, such that 95% of the total variance of the exponential covariance function are captured [59].

5.1. The impact of priors

Different priors are tested for this problem and we shall see how the priors affect the inference results. We specifically test the prior permeability fields associated with four different values of the correlation length α in (21): 5, 5/2, 5/4 and 5/8. To capture 95% of the total variance of the covariance function, we set the number of KL modes retained (the dimension of the parameter ξ) as: $M = 4$ for $\alpha = 5$, $M = 8$ for $\alpha = 5/2$, $M = 23$ for $\alpha = 5/4$ and $M = 73$ for $\alpha = 5/8$.

To generate posterior samples for comparison, the MCMC method described in Algorithm 1 is first performed with the forward model evaluated by the finite element method, which is referred to as the full MCMC method. We here draw $N = 10^6$ posterior samples using full MCMC with each of the above four priors. In all our numerical tests, the proposal distribution $\pi(\cdot|\xi^{(j)})$ on line 3 of Algorithm 1 (and on line 6 of Algorithm 4) is set to a multivariate Gaussian distribution with mean $\xi^{(j)}$ and covariance matrix $0.03^2 I$, where $\xi^{(j)}$ is the j -th sample in the Markov chain and $I \in \mathbb{R}^{M \times M}$ is an identity matrix. The acceptance rates (numbers of accepted samples divided by the total sample size) are 47%, 46%, 42% and 26% for $M = 4$, $M = 8$, $M = 23$ and $M = 73$ respectively, which indicates that the proposal is properly chosen [60]. In addition as expected, the acceptance rate decreases as the parameter dimension increases.

Fig. 2 shows the estimated posterior mean permeability fields generated by the sample means of full MCMC, each of which is defined as

$$\mathbf{E}_{\Xi^*}(a(x, \xi)) := \sum_{\xi \in \Xi^*} \frac{a(x, \xi)}{|\Xi^*|}, \quad (23)$$

where Ξ^* is the set of MCMC samples and $|\Xi^*|$ is its size. It is clear that, as the correlation length α reduces (the dimension of the parameter M increases), the estimated mean permeability field becomes visually similar to the actual field shown in Fig. 1(b). In particular, for a large correlation length $\alpha = 5$, while the prior is very smooth, the estimated posterior mean permeability is also too smooth compared with the actual field. For a smaller correlation, e.g., $\alpha = 5/8$, the prior becomes less smooth, and the estimated posterior mean permeability becomes more accurate. To assess the accuracy of the estimated posterior mean permeability, we introduce the following quantity of errors

$$\epsilon_{\Xi^*} := \|\mathbf{E}_{\Xi^*}(a(x, \xi)) - a_{\text{actual}}\|_0 / \|a_{\text{actual}}\|_0, \quad (24)$$

where a_{actual} is the actual permeability field shown in Fig. 1(b). Fig. 3 shows the errors with respect to the correlation lengths, where it is clear that small correlation lengths lead to small errors for our test problem. As discussed above, the dimension of the parameter depends on the correlation length: $M = 4$ for $\alpha = 5$, $M = 8$ for $\alpha = 5/2$, $M = 23$ for $\alpha = 5/4$ and $M = 73$ for $\alpha = 5/8$. This motivates us to focus on priors with small correlation lengths, which require high-dimensional parameterization.

5.2. Performance of RB-ANOVA surrogates

We here focus on the two high-dimensional cases in our test problem ($\alpha = 5/4$ with $M = 23$ and $\alpha = 5/8$ with $M = 73$), and test the RB-ANOVA-MCMC approach for these two cases. For comparison, an unadaptive version of RB-ANOVA-MCMC is also tested in addition to the adaptive RB-ANOVA-MCMC (Algorithm 4). The unadaptive version, which is referred to as

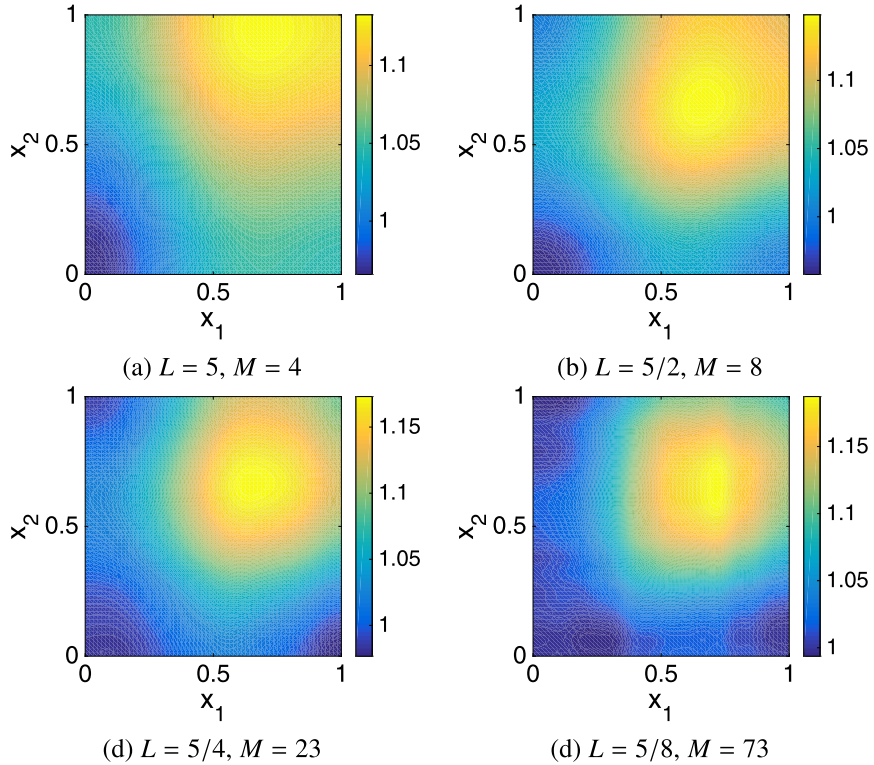


Fig. 2. Full MCMC results.

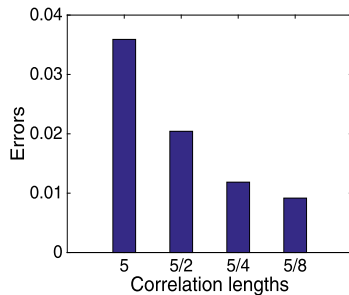


Fig. 3. Errors (ϵ_{Ξ^*}) w.r.t. correlation lengths (α).

the prior RB-ANOVA-MCMC method in the following, uses samples from the prior distribution to generate the RB-ANOVA model through Algorithm 2 and performs the MCMC iterations using this model. There are three tolerance parameters that need to be specified for generating the RB-ANOVA model in Algorithm 2: tol_{pod} for selecting singular vectors in POD on line 9 (details are discussed in Section 3.2), tol_{rb} on line 13 and tol_{anova} on line 24. Following the discussion of our work [37], we set them all to 10^{-4} in this work. For both prior and adaptive RB-ANOVA-MCMC, 10^3 samples are used to generate the RB-ANOVA model, i.e., $N_{model} = 10^3$ in Algorithm 4. Fig. 4 shows estimated mean and variance fields for the case $\alpha = 5/4$ with $M = 23$, generated by the three approaches: full MCMC, prior RB-ANOVA-MCMC, and adaptive RB-ANOVA-MCMC respectively with 10^6 samples. Here, the estimated mean fields are computed through (23), and the estimated variance fields are computed through

$$\mathbf{V}_{\Xi^*}(a(x, \xi)) := \sum_{\xi \in \Xi^*} \frac{1}{|\Xi^*|} \left(a(x, \xi) - \mathbf{E}_{\Xi^*}(a(x, \xi)) \right)^2, \quad (25)$$

where $\mathbf{E}_{\Xi^*}(a(x, \xi))$ is defined in (23) and Ξ^* is the posterior sample set generated by each of the three approaches. From Fig. 4, the estimated mean and variance fields generated by prior and adaptive RB-ANOVA-MCMC look very similar to those generated by full MCMC. For the case $\alpha = 5/8$ with $M = 73$, Fig. 5 shows that the estimated mean and variance fields generated by the three approaches are also very similar.

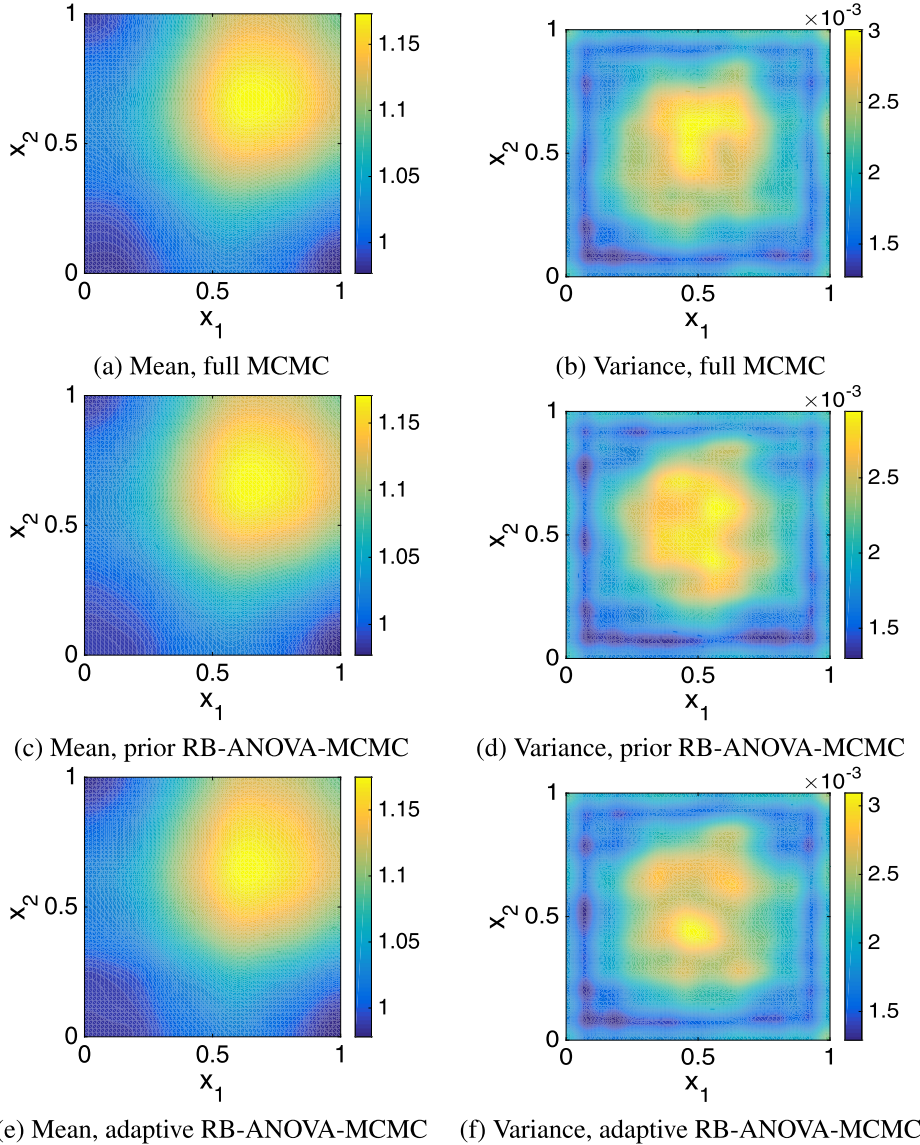


Fig. 4. Estimated mean and variance fields for $\alpha = 5/4$ with $M = 23$.

As discussed in Section 1, the main cost of the MCMC procedure comes from evaluating the forward model. For full MCMC, the forward model is evaluated using the finite element method, while it is evaluated using the RB-ANOVA model in our RB-ANOVA-MCMC approach. To assess the costs, we adopt the computational cost model for reduced basis methods developed in our recent work [37], which is based on counting relative sizes of linear systems (algebraic versions of (13) and (14)). In this cost model, for a given finite element degrees of freedom N_h , the cost for solving a full system (13) is defined to be a *cost unit*, which is assumed to be independent of the parameter ξ . The cost of solving a reduced problem (14) with size N_r is modelled by N_r/N_h . So, the cost of full MCMC is the number of forward model evaluations (see Algorithm 1), and the cost of our adaptive RB-ANOVA-MCMC is the sum of the costs for solving reduced systems (14) and full systems (13) involved Algorithm 4. In addition, it is clear that the cost of prior RB-ANOVA-MCMC is the sum of the costs in the construction procedure (Algorithm 2) and the costs of using Algorithm 3 to evaluate forward models in the MCMC iterations.

In addition, a standard combination of reduced basis methods and the MCMC method (Algorithm 1) is considered for comparison, which is referred to as RB-MCMC in the following. This RB-MCMC proceeds as follows. First, the snapshot corresponding to the initial sample in the Markov chain (see line 1 of Algorithm 1) is computed, and serves as the initial reduced basis. For each proposal sample (see line 3 of Algorithm 1), a reduced basis approximation solution and the corresponding error indicator (see (16)) is computed. If the value of the error indicator is smaller than the given tolerance (which is set to 10^{-4} in our test problems), the reduced basis approximation solution is used to compute the acceptance ratio (see line 4 of

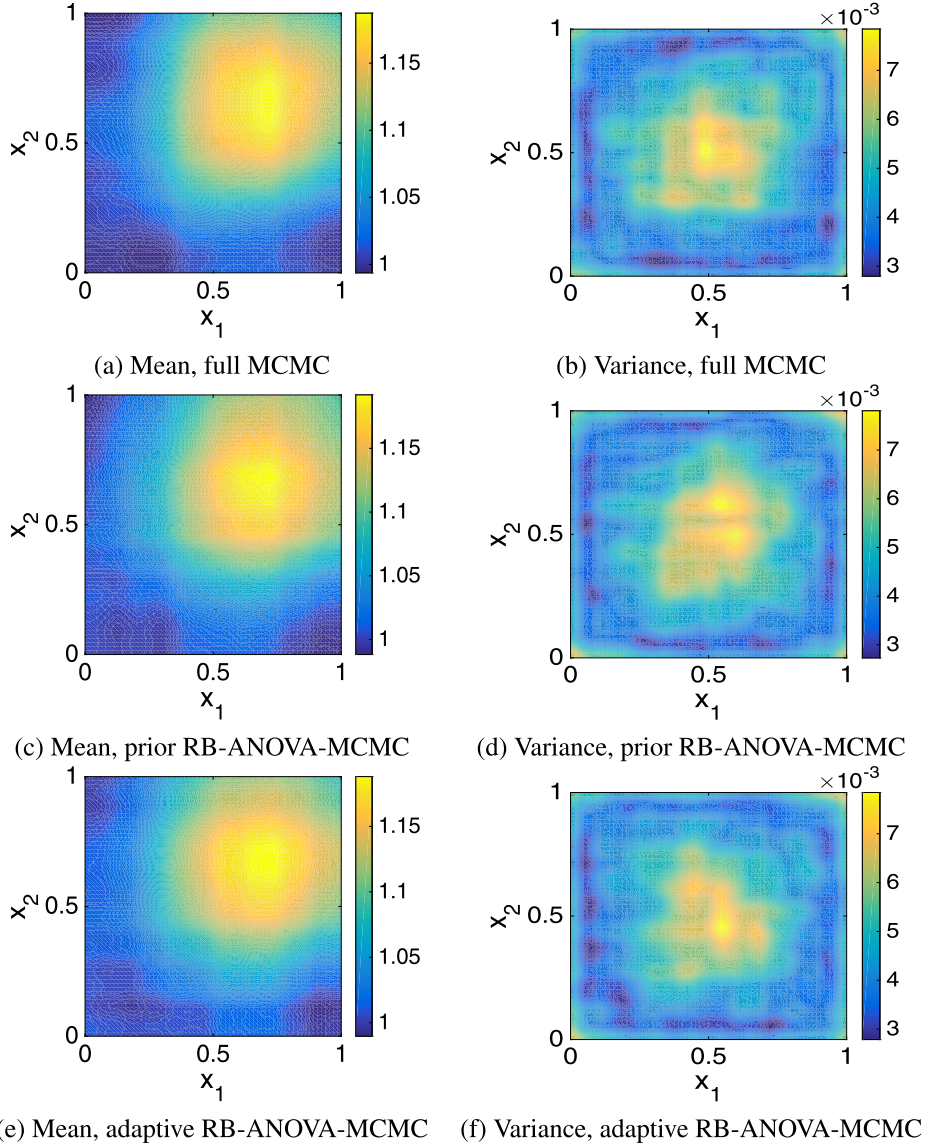


Fig. 5. Estimated mean and variance fields for $\alpha = 5/8$ with $M = 73$.

Algorithm 1); otherwise, the snapshot for this proposal sample is computed and used to compute the acceptance ratio, and the reduced basis is augmented with this snapshot. The cost of RB-MCMC is also assessed through the cost model discussed above.

Fig. 6 shows the costs with respect to the number of samples generated by the above methods. It is clear that, our adaptive RB-ANOVA-MCMC is the cheapest among these methods. From Fig. 6(a), to generate 10^6 posterior samples for the test problem with $M = 23$, the cost of adaptive RB-ANOVA-MCMC is around only one percent of the cost of full MCMC, and it is also much smaller than that of prior RB-ANOVA-MCMC. Note that the cost of full MCMC is slightly smaller than the sample size, since the prior distribution of the parameter ξ is set to a uniform distribution in $[-1, 1]^M$ and the proposed samples are rejected without evaluating the forward model if they are outside of $[-1, 1]^M$. For the case of $M = 73$ shown in Fig. 6(b), the cost of adaptive RB-ANOVA-MCMC to generate 10^6 samples is around ten percent of full MCMC, and it is less than half of the cost of prior RB-ANOVA-MCMC. In addition, the costs of RB-MCMC for both cases are similar to the costs of prior RB-ANOVA-MCMC. From both Fig. 6(a) and Fig. 6(b), at an early stage when the MCMC sample sizes are around 10^3 , adaptive RB-ANOVA-MCMC is more expensive than prior RB-ANOVA-MCMC. Moreover, for the case of $M = 73$ shown in Fig. 6(b), adaptive RB-ANOVA-MCMC is even more expensive than full MCMC at this early stage. The extra cost of adaptive RB-ANOVA-MCMC here comes from the reconstruction procedure of the RB-ANOVA model (see line 17 of Algorithm 4), where expensive finite element simulations are involved (see line 16 of Algorithm 2). However, as the MCMC iteration

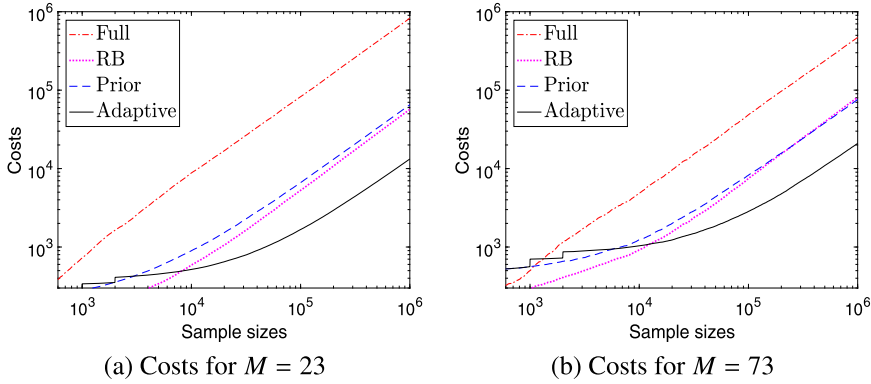


Fig. 6. Computational costs of full MCMC, RB-MCMC, prior RB-ANOVA-MCMC and adaptive RB-ANOVA-MCMC.

continues, the reconstruction procedure quickly stops, and the overall cost of adaptive RB-ANOVA-MCMC becomes much smaller than the costs of prior RB-ANOVA-MCMC and full MCMC.

To assess the accuracy of RB-ANOVA-MCMC, we evaluate the errors in mean and variance estimates through the following quantities,

$$\epsilon_{\text{mean}} := \|\mathbf{E}_{\Xi^*}(a(x, \xi)) - \mathbf{E}_{\text{ref}}\|_0 / \|\mathbf{E}_{\text{ref}}\|_0, \quad (26a)$$

$$\epsilon_{\text{var}} := \|\mathbf{V}_{\Xi^*}(a(x, \xi)) - \mathbf{V}_{\text{ref}}\|_0 / \|\mathbf{V}_{\text{ref}}\|_0, \quad (26b)$$

where $\mathbf{E}_{\Xi^*}(a(x, \xi))$ and $\mathbf{V}_{\Xi^*}(a(x, \xi))$ are defined in (23) and (25), and the reference mean estimate \mathbf{E}_{ref} and the reference variance estimate \mathbf{V}_{ref} are generated by full MCMC with 10^6 samples using (23) and (25). Fig. 7 and Fig. 8 show the errors of full MCMC, prior and adaptive RB-ANOVA-MCMC with respect to computational costs for the test problems with $M = 23$ and $M = 73$ respectively. It is clear that, the adaptive RB-ANOVA-MCMC method has the smallest errors when the costs are not very small. For very small cost values, e.g., around 10^3 in Fig. 8(a), the inefficiency of adaptive RB-ANOVA-MCMC (large errors in mean estimates) is caused by the reconstruction procedure, where snapshots need to be computed to reconstruct the RB-ANOVA model (see line 17 of Algorithm 4). As the MCMC iteration continues and the cost values increase, cost spent in the reconstruction procedure of the adaptive approach becomes invisible, and the adaptively constructed model becomes significantly efficient. For example, for the case with $M = 23$ shown in Fig. 7(a), to achieve an accuracy in estimating the mean with error smaller than 0.01, the cost required by adaptive RB-ANOVA-MCMC is less than 2000, which is less than a quarter of the cost required by prior RB-ANOVA-MCMC and is only around five percent of the cost of required full MCMC. From Fig. 7(b), to achieve an accuracy in estimating the variance with error smaller than 0.2 in this case, the cost of adaptive RB-ANOVA-MCMC is only around 1000, which is only around twenty percent of the cost required by prior RB-ANOVA-MCMC and is around two percent of the cost required by full RB-ANOVA-MCMC. Similarly, for the case with $M = 73$, Fig. 8(a) and Fig. 8(b) show that to achieve given accuracies in mean and variance estimates, adaptive RB-ANOVA-MCMC requires much less costs than prior RB-ANOVA-MCMC and full MCMC. In addition, Fig. 7 shows that for a given cost, the mean and the variance errors of RB-MCMC for the case $M = 23$ are typically smaller than the errors of prior RB-ANOVA-MCMC but larger than the errors of adaptive RB-ANOVA-MCMC, while Fig. 8 shows that the errors of RB-MCMC are very close to the errors of prior RB-ANOVA-MCMC for the case $M = 73$.

The number of ANOVA terms and the sizes of the reduced bases generated by adaptive RB-ANOVA-MCMC are shown in Table 1 and Fig. 9 respectively. Here, values associated with the prior distribution come from the initial RB-ANOVA model (see line 2 of Algorithm 4), and values associated with the posterior distribution come from the final RB-ANOVA model generated in the adaptive RB-ANOVA-MCMC procedure (see line 17 and line 19 of Algorithm 4). From Table 1, it can be seen that the ANOVA expansions generated by the prior distributions have both first and second order terms, while there is no third order term, which is consistent with the results in [34,37]. It can also be seen that, the ANOVA decompositions generated by the posterior distributions only have first order terms. Fig. 9 shows sizes of the reduced bases associate with each ANOVA term, where the indices are labelled in alphabetical order as follows: for any two different indices $t^{(j)}$ and $t^{(k)}$, $t^{(j)}$ is ordered before $t^{(k)}$ (i.e., $j < k$), if one of the following two cases is true: (a) $|t^{(j)}| < |t^{(k)}|$; (b) $|t^{(j)}| = |t^{(k)}|$ and for the smallest number $m \in \{1, \dots, |t^{(j)}|\}$ such that $t_m^{(j)} \neq t_m^{(k)}$, we have $t_m^{(j)} < t_m^{(k)}$ (where $t_m^{(j)}$ and $t_m^{(k)}$ are the m -th components of $t^{(j)}$ and $t^{(k)}$). From Fig. 9, while the sizes of the reduced bases associated with the posterior distributions are not larger than those associated with the prior distributions, there are many indices where the reduced bases associated with the posterior distributions have smaller sizes, e.g., for the indices labelled between twenty and seventy three in Fig. 9(b). These results are consistent with our expectation: ranges of posterior distribution samples are smaller than ranges of prior distribution samples, and the ANOVA index set and the reduced bases associated with the posterior distribution consequently have small sizes. These small sizes lead to the overall efficiency of adaptive RB-ANOVA-MCMC as shown in Fig. 7 and Fig. 8.

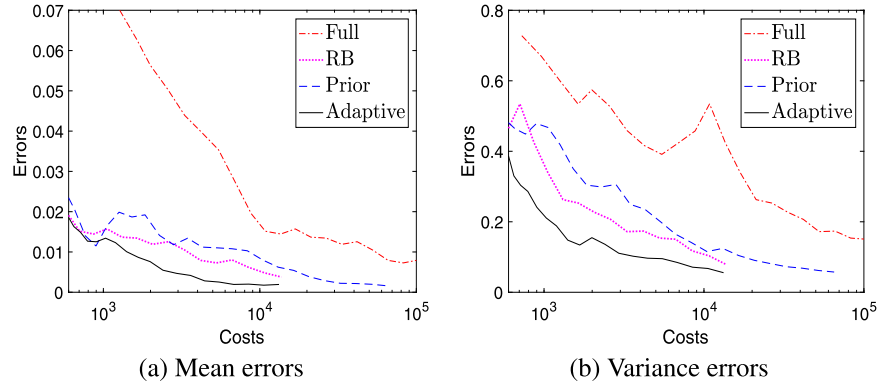


Fig. 7. Errors in mean and variance estimates (ϵ_{mean} and ϵ_{var}) of full MCMC, RB-MCMC, prior RB-ANOVA-MCMC and adaptive RB-ANOVA-MCMC, for $\alpha = 5/4$ with $M = 23$.

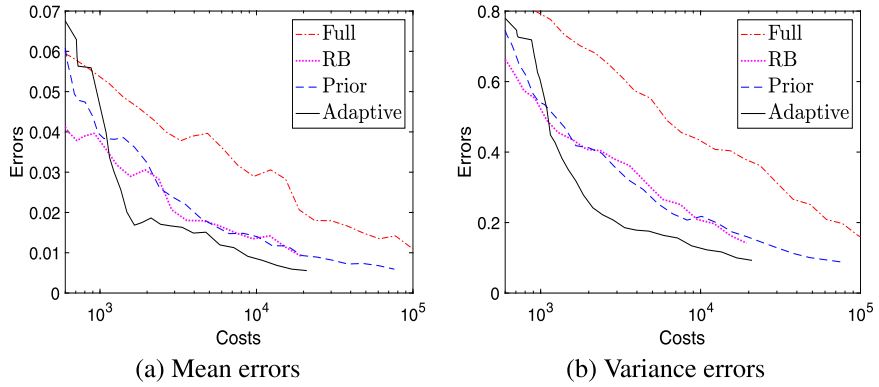


Fig. 8. Errors in mean and variance estimates (ϵ_{mean} and ϵ_{var}) of full MCMC, RB-MCMC, prior RB-ANOVA-MCMC and adaptive RB-ANOVA-MCMC, for $\alpha = 5/8$ with $M = 73$.

Table 1
Sizes of ANOVA index sets.

	$M = 23$		$M = 73$	
	$ \mathcal{J}_1 $	$ \mathcal{J}_2 $	$ \mathcal{J}_1 $	$ \mathcal{J}_2 $
Prior	23	28	73	45
Posterior	23	0	73	0

Table 2
Acceptance rates of full MCMC, prior RB-ANOVA-MCMC and adaptive RB-ANOVA-MCMC to generate 10^6 posterior samples.

M	Full	Prior	Adaptive
23	0.4175	0.4193	0.4159
73	0.2605	0.2656	0.2642

Finally, the acceptance rates for generating 10^6 posterior samples using the three approaches are shown in Table 2. It is clear that for both cases ($M = 23$ and $M = 73$), the acceptance rates of prior and adaptive RB-ANOVA-MCMC are consistent with the rates of full MCMC—they are the same up to two decimal places.

6. Conclusions

Conducting posterior-oriented model reduction is one of the fundamental concepts for solving high-dimensional Bayesian inverse problems. With a focus on ANOVA, this paper proposes a novel adaptive reduced basis ANOVA (RB-ANOVA) model with respect to posterior distributions to accelerate MCMC procedures. The first novelty of our new approach is the adaptive ANOVA decomposition based on the posterior mean estimates. It is known that the efficiency of the ANOVA decomposition is dependent on the choices of anchor points. Through adaptively updating the anchor point by posterior mean estimates

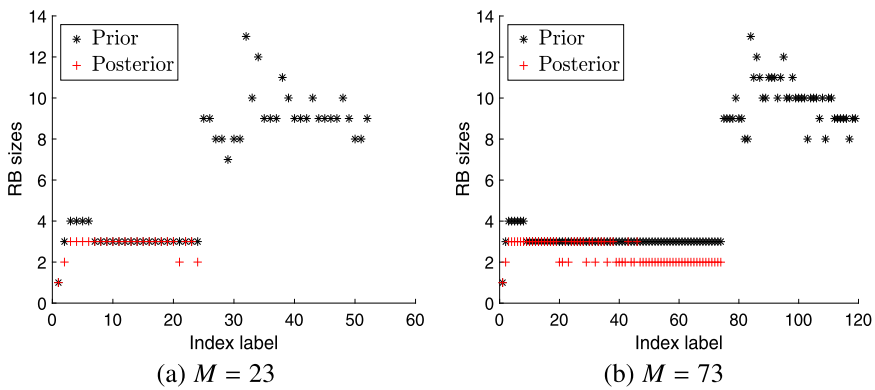


Fig. 9. Sizes of reduced bases for both test problems.

during MCMC iterations, an efficient ANOVA decomposition is obtained. Second, for all ANOVA terms, physical reduced bases are generated based on the posterior samples, which restricts the greedy algorithm to these samples so as to obtain optimal physical approximation bases for the Bayesian inversion problem. Numerical results demonstrate the overall efficiency of the proposed RB-ANOVA-MCMC algorithm. As our algorithm is based on ANOVA decomposition with a single anchor point, it currently can only be applied to Bayesian inversion problems with unimodal posterior distributions. For multimodal distributions, a possible solution is to do ANOVA decomposition with multiple anchor points. Designing and analyzing ANOVA decomposition with multiple anchor points for both forward and inverse UQ problems will be the focus of our future work.

Acknowledgements

Q. Liao is supported by NSFC under grant number 11601329 and J. Li is supported by the NSFC under grant number 11771289.

References

- [1] A. Tarantola, Inverse Problem Theory and Methods for Model Parameter Estimation, SIAM, 2005.
- [2] A. Tarantola Popper, Bayes and the inverse problem, *Nat. Phys.* 2 (8) (2006) 492–494.
- [3] J. Kaipio, E. Somersalo, Statistical and Computational Inverse Problems, Vol. 160, Springer Science & Business Media, 2006.
- [4] C.P. Robert, G. Casella, Monte carlo statistical methods, Springer Texts in Statistics, 2004.
- [5] J. Virieux, S. Operto, An overview of full-waveform inversion in exploration geophysics, *Geophysics* 74 (6) (2009) WCC1–WCC26.
- [6] W.W.-G. Yeh, Review of parameter identification procedures in groundwater hydrology: the inverse problem, *Water Resour. Res.* 22 (2) (1986) 95–108.
- [7] Y. Marzouk, D. Xiu, A stochastic collocation approach to Bayesian inference in inverse problems, *Commun. Comput. Phys.* 6 (4) (2009) 826–847.
- [8] Y.M. Marzouk, H.N. Najm, Dimensionality reduction and polynomial chaos acceleration of Bayesian inference in inverse problems, *J. Comput. Phys.* 228 (6) (2009) 1862–1902.
- [9] Y.M. Marzouk, H.N. Najm, L.A. Rahn, Stochastic spectral methods for efficient Bayesian solution of inverse problems, *J. Comput. Phys.* 224 (2) (2007) 560–586.
- [10] J.B. Nagel, B. Sudret, Spectral likelihood expansions for Bayesian inference, *J. Comput. Phys.* 309 (2016) 267–294.
- [11] L. Yan, L. Guo, Stochastic collocation algorithms using ℓ_1 -minimization for Bayesian solution of inverse problems, *SIAM J. Sci. Comput.* 37 (3) (2015) A1410–A1435.
- [12] L. Yan, T. Zhou, Adaptive multi-fidelity polynomial chaos approach to Bayesian inference in inverse problems, *J. Comput. Phys.* 381 (2019) 110–128.
- [13] L. Yan, T. Zhou, An adaptive multi-fidelity PC-based ensemble Kalman inversion for inverse problems, *Int. J. Uncertain. Quantif.* (2019) 205–220.
- [14] I. Bilionis, N. Zabaras, Solution of inverse problems with limited forward solver evaluations: a Bayesian perspective, *Inverse Probl.* 30 (1) (2013) 015004.
- [15] M.C. Kennedy, A. O'Hagan, Bayesian calibration of computer models, *J. R. Stat. Soc., Ser. B, Stat. Methodol.* 63 (3) (2001) 425–464.
- [16] H. Wang, J. Li, Adaptive Gaussian process approximation for Bayesian inference with expensive likelihood functions, arXiv preprint, arXiv:1703.09930.
- [17] X. Ma, N. Zabaras, An efficient Bayesian inference approach to inverse problems based on an adaptive sparse grid collocation method, *Inverse Probl.* 25 (3) (2009) 035013.
- [18] A. Narayan, T. Zhou, Stochastic collocation on unstructured multivariate meshes, *Commun. Comput. Phys.* 18 (2015) 1–36.
- [19] T. Cui, Y.M. Marzouk, K.E. Willcox, Data-driven model reduction for the Bayesian solution of inverse problems, *Int. J. Numer. Methods Eng.* 102 (5) (2015) 966–990.
- [20] D. Galbally, K. Fidkowski, K. Willcox, O. Ghattas, Non-linear model reduction for uncertainty quantification in large-scale inverse problems, *Int. J. Numer. Methods Eng.* 81 (12) (2010) 1581–1608.
- [21] C. Lieberman, K. Willcox, O. Ghattas, Parameter and state model reduction for large-scale statistical inverse problems, *SIAM J. Sci. Comput.* 32 (5) (2010) 2523–2542.
- [22] J. Wang, N. Zabaras, Using Bayesian statistics in the estimation of heat source in radiation, *Int. J. Heat Mass Transf.* 48 (1) (2005) 15–29.
- [23] C. Nguyen, G. Rozza, D.B.P. Huynh, A.T. Patera, Reduced basis approximation and a posteriori error estimation for parametrized parabolic PDEs: Application to real-time Bayesian parameter estimation, in: L. Tenorio, B. van Bloemen Waanders, B. Mallick, K. Willcox, L. Biegler, G. Biros, O. Ghattas, M. Heinkenschloss, D. Keyes, Y. Marzouk (Eds.), Large Scale Inverse Problems and Quantification of Uncertainty, in: Wiley Series in Computational Statistics, John Wiley & Sons, UK, 2010, pp. 151–178, Chapter 8, ePFL-IACS report 11.2008, http://augustine.mit.edu/methodology/methodology_technical_papers.htm.

- [24] E. Musharbash, F. Nobile, T. Zhou, Error analysis of the dynamically orthogonal approximation of time dependent random PDEs, *SIAM J. Sci. Comput.* 37 (2015) A776–A810.
- [25] M. Frangos, Y. Marzouk, K. Willcox, B. van Bloemen Waanders, *Surrogate and Reduced-Order Modeling: A Comparison of Approaches for Large-Scale Statistical Inverse Problems*, John Wiley & Sons, Ltd., 2010, pp. 123–149.
- [26] J. Li, A note on the Karhunen–Loëve expansions for infinite-dimensional Bayesian inverse problems, *Stat. Probab. Lett.* 106 (2015) 1–4.
- [27] R. Fisher, *Statistical Methods for Research Workers*, Oliver and Boyd, Berlin, 1925.
- [28] I. Sobol, Theorems and examples on high dimensional model representation, *Reliab. Eng. Syst. Saf.* 79 (2003) 187–193.
- [29] Y. Cao, Z. Chen, M. Gunzburger, ANOVA expansions and efficient sampling methods for parameter dependent nonlinear PDEs, *Int. J. Numer. Anal. Model.* 6 (2009) 256–273.
- [30] C. Winter, A. Guadagnini, D. Nychka, D. Tartakovsky, Multivariate sensitivity analysis of saturated flow through simulated highly heterogeneous ground-water aquifers, *J. Comput. Phys.* 217 (2009) 166–175.
- [31] Z. Gao, J.S. Hesthaven, On ANOVA expansions and strategies for choosing the anchor point, *Appl. Math. Comput.* 217 (2010) 3274–3285.
- [32] Z. Zhang, M. Choi, G. Karniadakis, Anchor points matter in ANOVA decomposition, in: *Spectral and High Order Methods for Partial Differential Equations*, in: *Lecture Notes in Computational Science and Engineering*, vol. 76, 2011, pp. 347–355.
- [33] X. Ma, N. Zabaras, An adaptive high-dimensional stochastic model representation technique for the solution of stochastic partial differential equations, *J. Comput. Phys.* 229 (2010) 3884–3915.
- [34] X. Yang, M. Choi, G. Lin, G.E. Karniadakis, Adaptive ANOVA decomposition of stochastic incompressible and compressible flows, *J. Comput. Phys.* 231 (2012) 1587–1614.
- [35] J. Foo, G. Karniadakis, Multi-element probabilistic collocation in high dimensions, *J. Comput. Phys.* 229 (2010) 1536–1557.
- [36] J.S. Hesthaven, S. Zhang, On the use of ANOVA expansions in reduced basis methods for high-dimensional parametric partial differential equations, *J. Sci. Comput.* (2019), in press, <https://doi.org/10.1007/s10915-016-0194-9>.
- [37] Q. Liao, G. Lin, Reduced basis ANOVA methods for partial differential equations with high-dimensional random inputs, *J. Comput. Phys.* 317 (2016) 148–164.
- [38] H. Cho, H.C. Elman, An adaptive reduced basis collocation method based on PCM ANOVA decomposition for anisotropic stochastic PDEs, *Int. J. Uncertain. Quantificat.* 8 (2018) 193–210.
- [39] Z. Zhang, M. Choi, G. Karniadakis, Error estimates for the ANOVA method with polynomial chaos interpolation: tensor product functions, *SIAM J. Sci. Comput.* 34 (2) (2012) A1165–A1186.
- [40] L. Sirovich, Turbulence and the dynamics of coherent structures, part I: coherent structures, *Q. Appl. Math.* 45 (1987) 561–571.
- [41] P. Holmes, J.L. Lumley, G. Berkooz, *Turbulence, Coherent Structures, Dynamical Systems and Symmetry*, 1996, Cambridge, New York.
- [42] M. Gunzburger, J. Peterson, J. Shadid, Reduced-order modeling of time-dependent PDEs with multiple parameters in the boundary data, *Comput. Methods Appl. Mech. Eng.* 196 (2007) 1030–1047.
- [43] K. Veroy, D. Rovas, A. Patera, A posteriori error estimation for reduced-basis approximation of parametrized elliptic coercive partial differential equations: “Convex Inverse” bound conditioners, *ESAIM Control Optim. Calc. Var.* 8 (2002) 1007–1028.
- [44] N. Nguyen, K. Veroy, A. Patera, Certified real-time solution of parametrized partial differential equations, in: S. Yip (Ed.), *Handbook of Materials Modeling*, Springer, 2005, pp. 1523–1558.
- [45] B. Haasdonk, M. Ohlberger, Reduced basis method for finite volume approximations of parametrized linear evolution equations, *ESAIM: Math. Model. Numer. Anal.* 42 (2008) 277–302.
- [46] T. Bui-Thanh, K. Willcox, O. Ghattas, Model reduction for large-scale systems with high-dimensional parametric input space, *SIAM J. Sci. Comput.* 30 (2008) 3270–3288.
- [47] S. Boyaval, C.L. Bris, T. Lelièvre, Y. Maday, N. Nguyen, A. Patera, Reduced basis techniques for stochastic problems, *Arch. Comput. Methods Eng.* 17 (2010) 1–20.
- [48] A. Patera, G. Rozza, Reduced basis approximation and a posteriori error estimation for parametrized partial differential equations, in: *MIT Pappalardo Graduate Monographs in Mechanical Engineering*, 2007, in press, version 1.0, copyright MIT 2006–2007.
- [49] A. Quarteroni, A. Manzoni, F. Negri, *Reduced Basis Methods for Partial Differential Equations*, Springer International Publishing, Switzerland, 2016.
- [50] H. Elman, Q. Liao, Reduced basis collocation methods for partial differential equations with random coefficients, *SIAM/ASA J. Uncertain. Quantificat.* 1 (2013) 192–217.
- [51] C. Newsum, C. Powell, Efficient reduced basis methods for saddle point problems with applications in groundwater flow, *SIAM/ASA J. Uncertain. Quantificat.* 5 (1) (2017) 1248–1278.
- [52] Q. Guan, M. Gunzburger, C.G. Webster, G. Zhang, Reduced basis methods for nonlocal diffusion problems with random input data, *Comput. Methods Appl. Mech. Eng.* 317 (2017) 746–770.
- [53] J. Li, Y.M. Marzouk, Adaptive construction of surrogates for the Bayesian solution of inverse problems, *SIAM J. Sci. Comput.* 36 (3) (2014) A1163–A1186.
- [54] D. Braess, *Finite Elements*, Cambridge University Press, London, 1997.
- [55] H. Elman, D. Silvester, A. Wathen, *Finite Elements and Fast Iterative Solvers*, Oxford University Press, New York, 2005.
- [56] R. Ghanem, P. Spanos, *Stochastic Finite Elements: A Spectral Approach*, Dover Publications, New York, 2003.
- [57] I. Babuška, F. Nobile, R. Tempone, A stochastic collocation method for elliptic partial differential equations with random input data, *SIAM J. Numer. Anal.* 45 (2007) 1005–1034.
- [58] H. Elman, C. Miller, E. Phipps, R. Tuminaro, Assessment of collocation and Galerkin approaches to linear diffusion equations with random data, *Int. J. Uncertain. Quantificat.* 1 (2011) 19–34.
- [59] C. Powell, H. Elman, Block-diagonal preconditioning for spectral stochastic finite-element systems, *IMA J. Numer. Anal.* 29 (2009) 350–375.
- [60] G.O. Roberts, J.S. Rosenthal, Optimal scaling for various Metropolis-Hastings algorithms, *Stat. Sci.* 16 (2001) 351–367.